JET–P(97)29

# Operation at High Performance in Optimised Shear Plasmas in JET

A.C.C. Sips, C.D. Challis, G.A. Cottrell, L-G Eriksson, C. Gormezano, C. Gowers, C.M. Greenfield[1], J.C.M de Haas, M. von Hellerman, G.T.A. Huysmans, A. Howman, R. König, E.A. Lazarus[2], T. Luce[1], P. Nielsen, D. O'Brien, B.W. Rice[3], G. Sadler, F.X. Söldner, M.F. Stamp, E.J. Strait[1], B.J.D. Tubbing, M. Wade[2], and D.J. Ward.

JET Joint Undertaking, Abingdon, Oxfordshire, OX14 3EA, UK.
[1]General Atomics, San Diego, USA,
[2]Oak Ridge National Laboratory, Oak Ridge, Tennessee, USA,
[3]Lawrence Livermore National Laboratory, California, USA.

Preprint of a paper to be submitted for publication in
Plasma Physics and Controlled Fusion

October 1997

**ABSTRACT**

*Heating during the early part of the current rise phase gives a low or negative magnetic shear (=r/q(dq/dr)) in the centre of JET plasmas. Under these conditions the confinement improves with high additional heating power heating during the current ramp-up phase of the discharge. The reduction in the transport manifests itself as a peaking of the profiles with a large gradient region near r/a=0.55. The best discharges have no transport barrier at the edge of the plasma (L-mode). This allows central power deposition by the neutral beams in JET. A control of the plasma pressure, using feedback of the additional heating power in real-time, minimises the impact of MHD instabilities. As a result, these discharges achieve the highest D-D neutron rates in JET;* $S_n=5.6x10^{16}$ *neutrons/s, with* $n_{e0}\approx 6x10^{19}\ m^{-3}$, $T_{e0}\approx 12$ *keV and* $T_{i0}\approx 26$ *keV.*

## 1. INTRODUCTION

The exploration of improved confinement regimes in tokamaks is one of the major topics in the present fusion research program. Regimes with enhanced performance could lead to a significant reduction in the required plasma current for a reactor. This allows a reduction in the size and cost of a future fusion power plant.

The most significant regime of enhanced confinement is the H-mode, which has a transport barrier just inside the separatrix of the plasma. High performance regimes, which use the H-mode to maximise the global confinement generally tend to have broad pressure profiles. In these plasmas, MHD events limit the rise in central density, temperature and fusion performance, which scales as $n_i^2 T_i^2$. The most common MHD events are sawteeth, or ELMs and MHD modes near the edge of the plasma driven by the edge pressure and current density [1,2].

Alternatively, regimes with improved energy and particle confinement in the centre provide a route for enhanced performance, provided that the increased pressure peaking does not compromise the MHD stability of the plasma. Generally these scenarios have central q values in excess of 1 to eliminate sawtooth instabilities. Many tokamaks have concentrated the research on heating during the current rise phase of the discharge. JET obtained enhanced core performance by deep pellet fuelling of non-sawtoothing plasmas and subsequent heating of the core [3]. Analysis indicated low and reversed magnetic shear in the centre associated with a reduction in the transport [4]. TFTR [5], DIII-D [6] and JT-60 [7] use neutral beam heating during the current ramp phase to slow down the current diffusion to obtain a reversed magnetic shear. These experiments show an improved confinement with strong additional heating of the centre of the plasma. Provided that MHD instabilities are avoided, this regime with peaked pressure profiles gives a route to high fusion performance.

In the 1994/1995 campaign, JET obtained central electron temperatures of more than 10 keV with low power LHCD in the early part of the current rise phase [8]. This is similar to results reported by PLT [9] and TORE-SUPRA [10]. Transport analyses indicate a strong reduction of the electron thermal diffusivity. Neutral beam injection into these low density plasmas was not possible due to shine-through power loading of in-vessel components. Subsequent modifications to the in-vessel protection have largely removed this restriction for the present operational campaign (1996/1997).

In this paper we present new results on the formation of internal transport barriers obtained with high neutral beam power. We will focus on the operation with strongly peaked pressure profiles, and show the realisation of maximum performance by controlling the central pressure to avoid MHD instabilities.

## 2. CURRENT RISE SCENARIO

Experiments were performed in lower single null X-point configurations at 3.4 Tesla, with $I_p \leq 3.3$ MA and $q_{95} \geq 3.8$, after the installation of the Mk II divertor [11]. JET obtains high performance during the current rise with the scenario shown in Figure 1. This typical scenario starts with a low voltage breakdown. In the first second of the discharge, LHCD provides off-

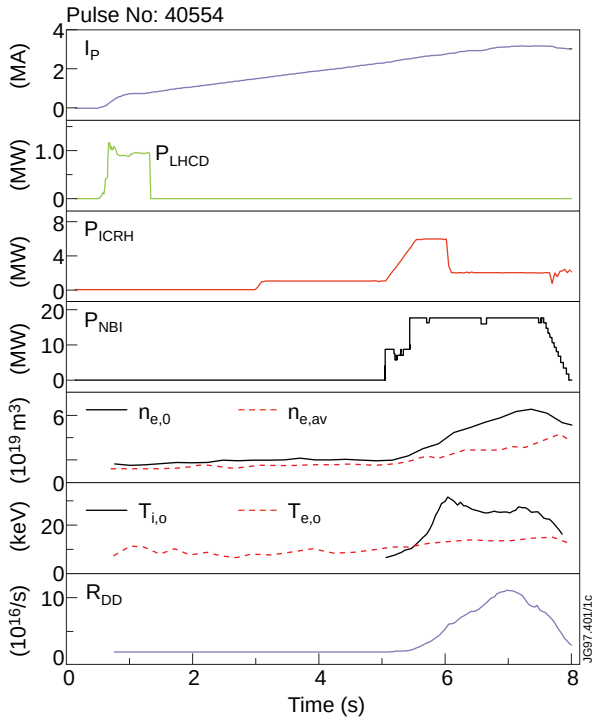


*Figure 1 Breakdown and initial current rise with LHCD assist. The X-point phase starts at 1.3 seconds. The current rise is at 0.4 MA/s keeping the density as low as possible. ICRH preheats of the target discharge. The main heating starts at 5 seconds.*

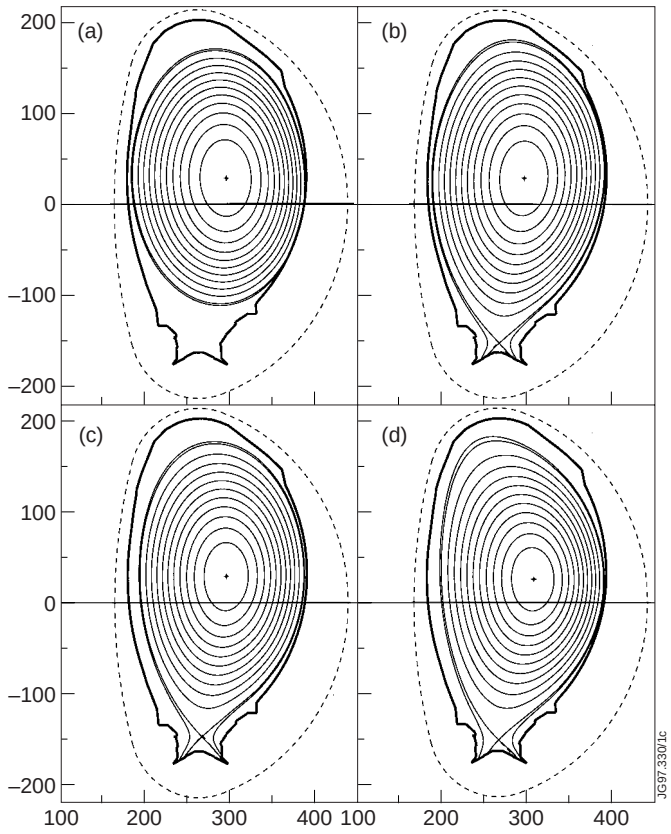


Figure 2 Plasma cross section at several different stages of the discharge. The plasma starts with the maximum aperture after breakdown (a), and the X-point forms at 1 MA at 1.3 seconds (b). The target plasma has a low triangularity and the outer strike point close to the divertor cryo-pump to maintain an L-mode edge (c). During the high performance phase the triangularity increases to $\delta_{upper} = 0.35$ and $\delta_{lower} = 0.30$ (d).

axis current drive and increases the electron temperature. The current rise rate is 0.4 MA/s with an X-point formation at t=1.3 seconds at 1 MA. ICRH starts 3 seconds after breakdown at a level of 1 MW and increases the electron temperature to 6 keV, using Hydrogen minority heating with the resonance near the centre. Low density operation ($n_{e,\,av} < 1.0\ 10^{19}\ m^{-3}$) is essential for the formation of the target plasma at t=5.0 seconds when $I_p$ reaches 2.5 MA. This scenario differs from other tokamak experiments that use preheating by neutral beams.

Neutral beam ( $\leq 20$ MW) and ICRF ($\leq 10$ MW) heating of the target plasma can lead to a strong peaking of the central pressure with the edge of the plasma remaining in L-mode [12]. The use of a low target density ($n_{e,\,av} = 0.6x10^{19}\ m^{-3}$) density, a current ramp of 0.4 MA/s and a low triangularity at the start of the main heating ($\delta_{upper} = 0.05$ and $\delta_{lower} = 0.25$, Figure 2) delay the onset of the H-mode. In addition, the good core confinement reduces the loss power to the edge, allowing the L-mode to be sustained at input powers well in excess of the H-mode power threshold for these plasmas ($\approx 8$ MW). The lowest power required for the formation of the transport barrier is 11 MW NBI combined with 6 MW ICRH.

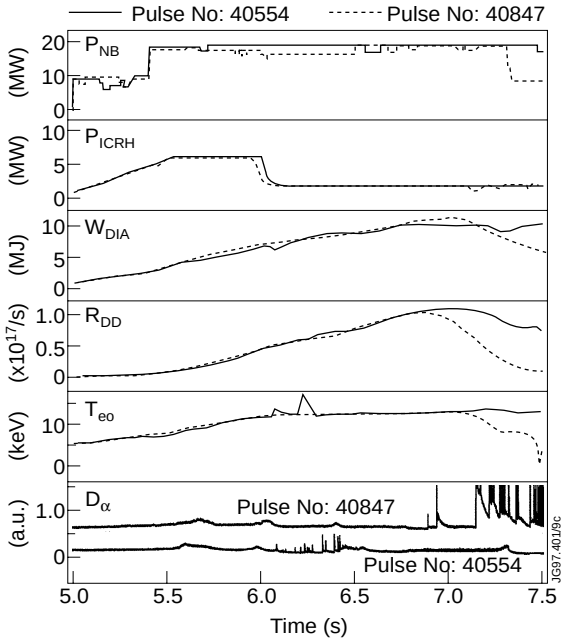


Figure 3 With control of the additional heating power the discharge becomes fairly reproducible. Pulse 40554 has conditioned first walls while pulse 40847 is just after a vessel opening. This regime may not sensitive to the edge conditions.

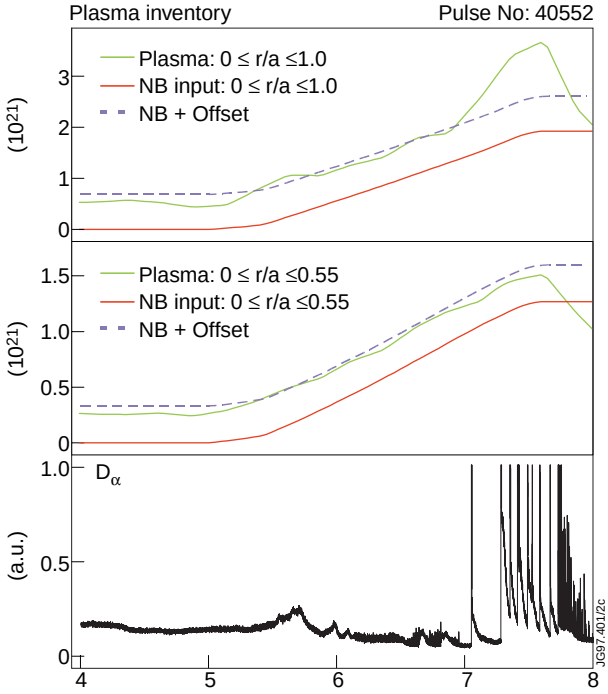


Figure 4 Inside the transport barrier (r/a < 0.55) the particle inventory rises with the neutral beam fuelling. During the H-mode the total particle inventory rises sharply. This indicates an increase in edge density due to improved confinement at the edge. This transport barrier at the edge also accumulates particles from the recycling sources.

Pulse 40554, shown in Figure 1, has the highest D-D fusion reaction rate in JET with $S_n = 5.6x10^{16}$ neutrons/s. A TRANSP calculation of the neutron rate is consistent with the measurement to within 10% indicating a 67% thermonuclear emission. The heating power at peak performance is 18.5 MW NBI and 2 MW ICRH giving a stored energy of 10.5 MJ. This is an enhancement over ITER-89 L-mode scaling of 2.2. The central density reaches $6 \times 10^{19}$ $m^{-3}$ with $T_{e0} \approx 12$ keV and $T_{i0} \approx 26$ keV. Pulse 40847 with $S_n = 5.4x10^{16}$ neutrons/s is a close second in maximum neutron yield demonstrating the reproducibility of this regime. The evolution of the discharge is nearly identical to pulse 40554 by applying the same heating waveform (Figure 3).

One of the key elements during the high performance phase is the evolution of the density profile. Positioning the outer strike point close to the divertor cryo pump maintains a low edge density. The improved core confinement results in a continuous increase of the central density. A TRANSP simulation of the discharge [13] indicates that the plasma particle inventory in the centre rises by the number of neutral beam particles deposited inside the barrier [14] (Figure 4). Transition of the discharge to an ELM free H-mode improves the particle confinement of the edge and leads to a rapid rise of the total plasma particle inventory. This regime obtains the maximum performance with an L-mode edge and peaked pressure profiles.

## 3. TRANSPORT BARRIER

The reduction in core transport manifests itself as a rapid increase of the ion temperature in the first second of the heating phase (Figure 5). A region with a large gradient in the ion temperature profile starts in the centre and moves out to r/a=0.55 with constant heating power. For the ion temperature this gradient can build up to $\nabla T_i \approx 70$keV/m. This transport barrier is also observed in the toroidal rotation ($\omega_\varphi$) profiles, electron temperature profiles and electron density profiles (Figure 6). Their gradients build up to a maximum of $\nabla\omega_\varphi \approx 500$krads$^{-1}$/m, $\nabla T_e \approx 35$keV/m and $\nabla n_e \approx 1.0x10^{20}/m^4$ respectively.

ICRF heats the centre of the discharge during the formation of the transport barrier and the subsequent high performance phase. The resonance is close to the magnetic axis using Hydrogen minority heating (51.2 MHz at 3.4 Tesla). The increase of the ion temperature allows an increased damping of the ICRH on the bulk ions due to finite larmor radius effects. TRANSP calculations show that with a typical hydrogen concentration of 1% and ion temperature around 30 keV the bulk ions absorb up to 60% of the ICRH power [14]. The ICRH power initially maintains a high electron temperature without applying sufficient power to trigger an H-mode. The formation of internal transport barrier with high ion temperatures allows control of the central ion pressure with ICRH.

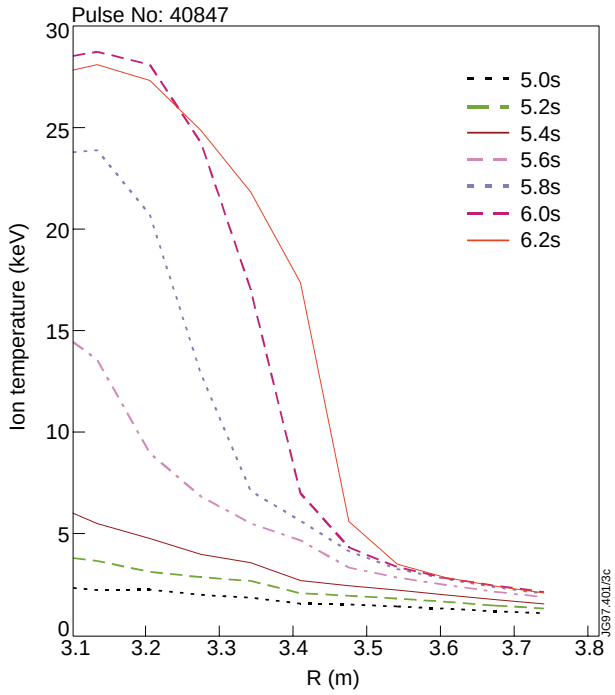


Figure 5 Increase in central ion temperature in the first second of additional heating. The additional heating start at 5.0 seconds with the maximum neutral beam power starting at 5.4 seconds. The transport barrier forms near the centre and then expands to larger radii.

An EFIT [15] reconstruction of the target q-profile required for the formation of the transport barrier gives q=2 near the centre with low magnetic shear. The EFIT reconstruction uses data from magnetic probes at the boundary, 1 channel of Faraday rotation measurements close to the centre of the plasma and the measured pressure profile. The estimated uncertainty is ±0.5 for the central q values, therefore the sign of the magnetic shear and the optimum q-profile in the centre are undetermined. JET obtained the optimum target q-profile in an empirical way. This was the only route available to optimise this regime without an accurate q profile diagnostic such as a Motional Stark Effect system. For example, a continuation of the current ramp without neutral beam leads to error field modes at low $q_{95}$. In addition later heating times require more input power to reduce the core transport and trigger early H-mode transitions (Figure 7). On the other hand, a start of the heating well before t=5.0 s or to use of more LHCD also increases the required power for barrier formation.

## 4. PERFORMANCE WITH PEAKED PRESSURE PROFILES

Just after the barrier formation the pressure peaking reaches its maximum. At this time the discharge is most susceptible to MHD instabilities. It is important not to ‘overheat’ the centre before the barrier has moved out sufficiently. This implies a narrow operating window for the

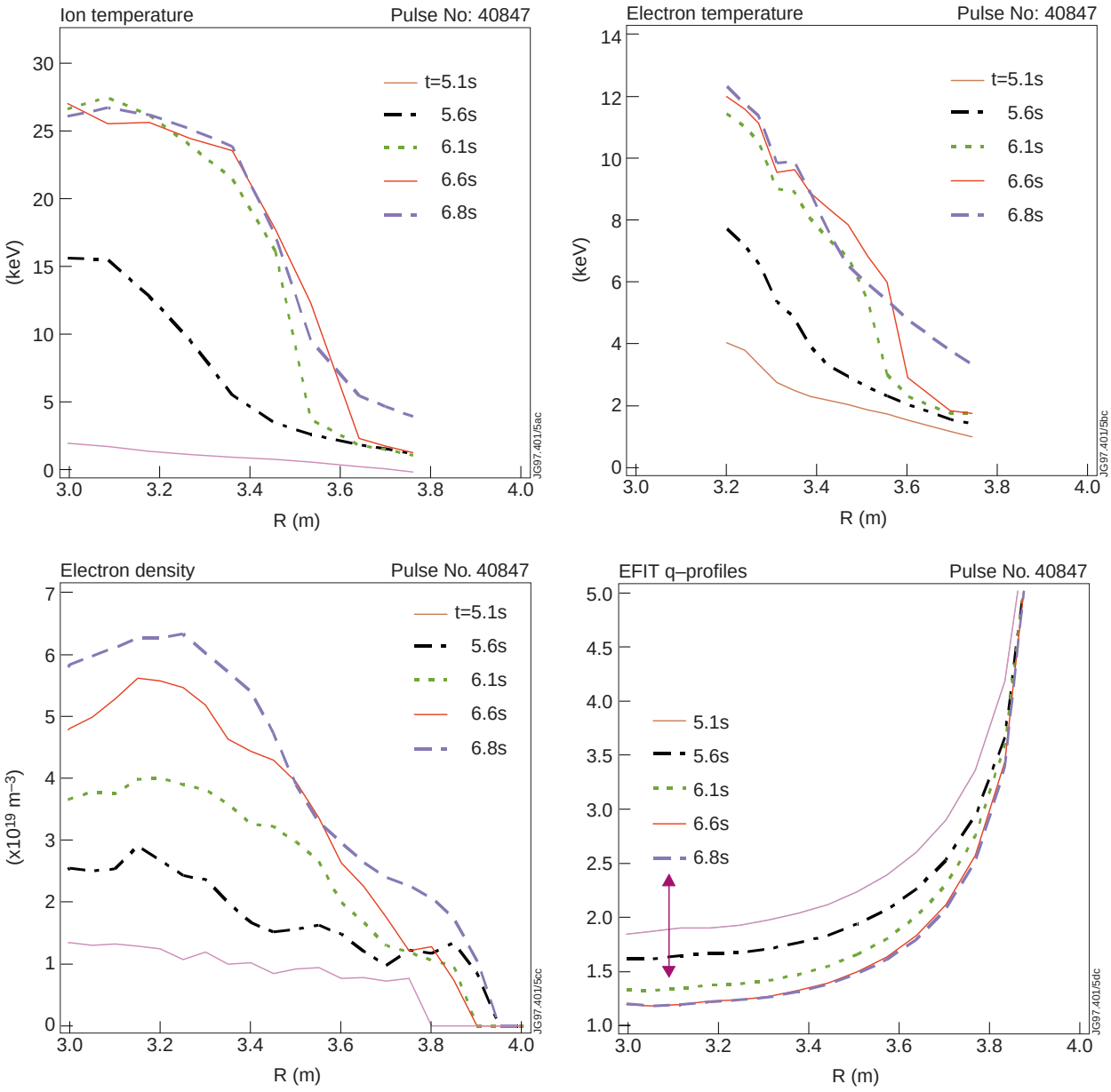


Figure 6 Shown is the evolution of the profiles during the high performance phase. ICRH and neutral beam heating start at t=5.0 s and peak performance is at t=6.8 s. The central density increases with the neutral beam fuelling. The EFIT q-profiles indicate a drop in the central q values during the heating phase, within the uncertainties the sign of the shear is undetermined.

additional heating power, which must be sufficient to maintain the barrier, without providing too much power as to provoke a disruption. The difference between these input powers is 4-6 MW. To stay in this narrow operational space requires a control of the additional heating power using a real time feedback algorithm. The main control parameter is the D-D fusion reaction rate ($R_{DD}$). Typically, the ICRH power steps down from 6 MW to 2 MW when $R_{DD}$ reaches $4x10^{16}$/s, at around t=6.0 seconds. An $R_{DD}$ waveform request controls the neutral beam power. The

optimum waveform is slightly lower than the $R_{DD}$ obtained in disruptive discharges. A controlled rise of $R_{DD}$ at a level slightly below the disruptive limit, provides stability to obtain a high instantaneous and integrated neutron yield.

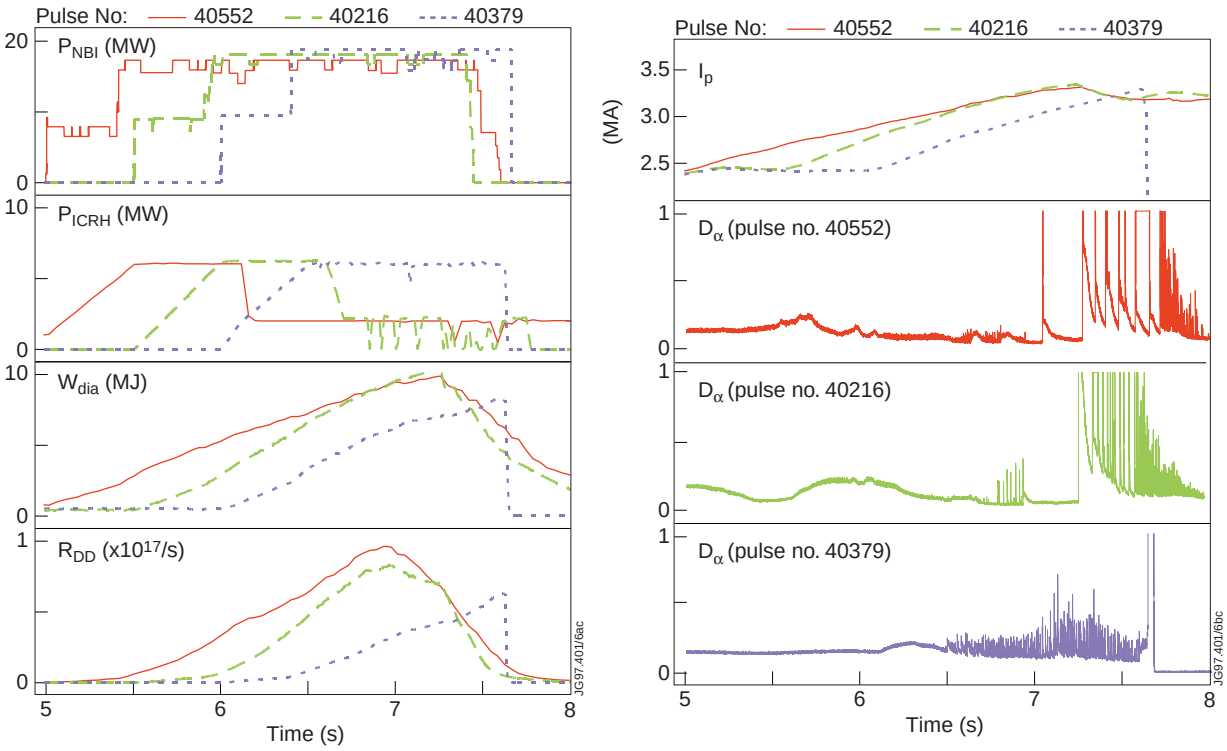


Figure 7 Heating at different times during the discharge. A start of the heating at 5.0 seconds gives the best performance. Starting the heating later triggers the H-mode early and requires faster current ramps to try to suppress the H-mode transition.

For this regime, we relate the D-D fusion reaction rate to the product of $(W_{dia})^2$ and peaking factor of the density profile; $R_{DD} = 400\ (W_{dia})^2\ (nel_{centre}/\ nel_{edge})$. A calculation of the ratio of a central channel ($nel_{centre}$) and edge channel ($nel_{edge}$) of the interferometer gives the density peaking factor in real-time. The use of this $R_{DD}$ substitute in the power feedback algorithm provides a faster response to profile changes and is insensitive to the plasma composition. A rapid loss of the density peaking when the barrier weakens leads to the application of the maximum available power to restore the improved confinement.

More detailed analyses of pulse 40847 use the MISHKA-1 ideal MHD code to determine the stability limit for the n=1 mode [16]. The calculations rely on pressure profiles and q-profiles from TRANSP. The results show a very low limit on $\beta_N$ of about 1.0 starting at t=5.5s, when $p_0/$ <p> reaches 8 (Figure 8). The pressure profile broadens when the transport barrier moves outwards. In addition, a timely reduction of the additional heating at 6.0 seconds allows the discharge stays within the stable region. With the reduction of the peaking factor the marginal

value for $\beta_N$ increases to 1.8 at t=7.0 seconds. The avoidance of disruptions, by controlling the central pressure, is consistent with the calculation of the MHD stability limits.

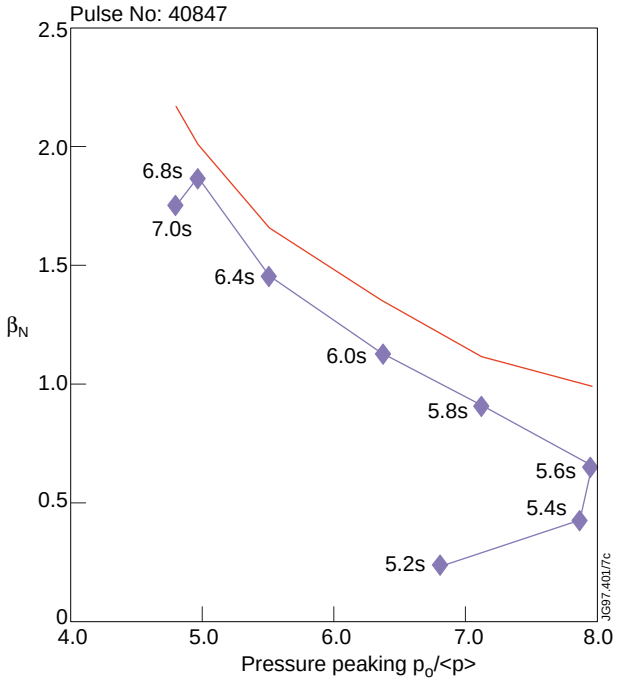


Figure 8 The stability of the discharge depends on the pressure peaking. The solid curve gives the stability limit for n=1 mode. The solid-dot curve gives the evolution of the discharge. The pressure profile broadens due a widening of the region of improved confinement in the first second. A reduction of the heating power around t=6.0 seconds keeps the discharge in the stable region.

The maximum $\beta_N$ obtained in these plasmas approaches 1.8 at 3.3MA/3.4T. The expansion of the region of improved confinement stops after t=6.0 seconds and the pressure gradient at r/a =0.55 continues to increase. High frequency MHD modes gradually degrade the internal transport barrier despite the control of the additional heating power to minimise the effects of MHD instabilities. The location of these modes with n=2-7 is near the position of the steep pressure gradient [17]. The increased outward heat flow normally triggers an H-mode, which improves the global confinement, but the pressure in the core continues to decline.

## 5. DISCUSSION AND CONCLUSIONS

The optimised shear regime in JET has shown rapid progress in the 1996/1997 experimental campaign. Initial experiments observed spontaneous peaking of the pressure profile at 15 MW of NBI and 6-8 MW ICRH. The increase of the central pressure was in conjunction with reduced ELM activity. By avoiding the formation of an edge transport barrier, discharges obtained a

prompt and controlled improvement of the confinement in the centre. At this stage of the experimental campaign, most plasmas ended with a fast disruption, with growing n=1, m=1 and n=2, m=1 activity in the core before the collapse. The use of a low voltage breakdown allowed an increase of the triangularity during the main heating phase; from $\delta_{upper} = 0.05$ and $\delta_{lower} = 0.25$ to $\delta_{upper} = 0.35$ and $\delta_{lower} = 0.30$. By doing this, the increase of electron density in the centre became more pronounced at the same additional heating power. An increase in plasma current from 3 MA to 3.3 MA improved the performance further. Finally, a modest preheating with ICRH at 1 MW provided a more reliable target plasma. With the avoidance of MHD instabilities the regime achieved record performance. The fusion reactivity is substantially higher for a given stored energy, compared to the Hot-ion ELM free regime in JET [18] (Figure 9).

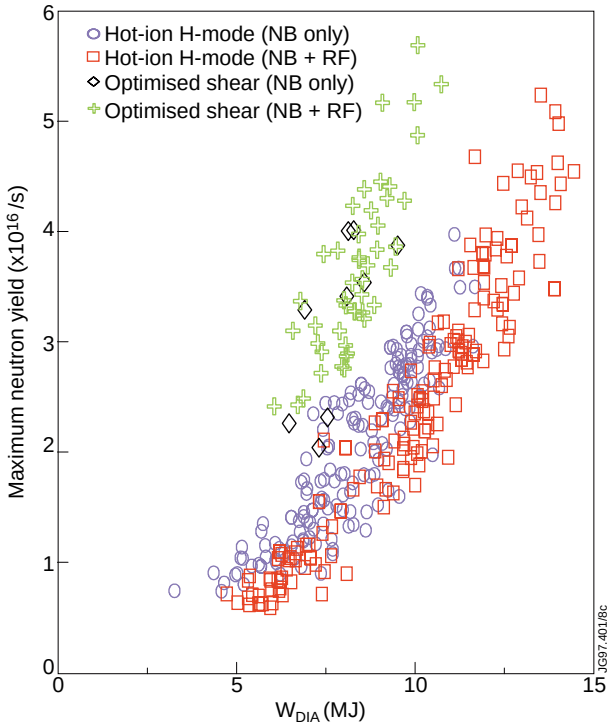


Figure 9 A regime with peaked pressure profiles obtains a substantially higher fusion reactivity for a given stored energy. The performance of the optimised shear regime compares favourably to the Hot-ion ELM free regime in JET (Mk II data only).

MHD stability calculations and the observations in DIII-D [19] indicate that the fusion power increases with broader pressure profiles (peaking factors < 4). For JET, two options are available to achieve this: An expansion of the improved core transport region to beyond radius r/a = 0.55, or adding an edge transport barrier by triggering an H-mode. The first option relies on a change of the target plasma. During the main heating phase, the use of different ICRH resonance positions can spread the power deposition or LHCD can provide additional off-axis current drive. This clearly needs more development in JET.

Most discharges trigger an H-mode transition when MHD events weaken the transport barrier, associated with the increased energy flow to the edge. In these cases the core continues to collapse, despite an increase of the neutral beam power by the feedback algorithm. Some discharges do make a transition to the H-mode without a collapse of the core. However, the rise in the central pressure stops within 0.2 to 0.4 seconds. The increase in edge density does broaden the neutral beam power deposition, reducing the power flow to the core by 10%-15%. Second, the gradient at the transport barrier reduces significantly, maybe weakening the stabilising mechanism for the enhanced transport. Third, the increase in edge current density alters the evolution of the current density profile in time. However, none of the above give a clear cause for the decline of the centre and require more detailed analysis. A few discharges have small ELMs to control the edge density and edge pressure gradients do sustain the peaked pressure in the core. Operation in this regime is difficult as it requires a delicate balance between the central power deposition required to keep the improved confinement and the control of the edge to keep the ELMs small. This regime has the potential for steady state operation but needs more development.

In conclusion, plasmas have an improvement in the central confinement with high power heating during the current rise phase of the discharge. This current rise is at low density in single null X-point configurations. In addition, the use of LHCD current drive and ICRH preheating result in target plasmas with low or negative magnetic shear in the centre. With neutral beam ($\leq$ 20 MW) and ICRF ($\leq$ 10 MW) heating the reduction in transport manifests itself by a peaking of the profiles with a large gradient region near r/a = 0.55. During the high power phase a control of the pressure peaking minimises the effect of MHD instabilities. This requires feedback on the D-D fusion reaction rate using the additional heating power, which allows the barrier to move out and the pressure profile to broaden. Discharges without an edge density pedestal have central neutral beam power deposition and give the highest D-D neutron rates in JET; $S_n$=5.6x$10^{16}$ n/s, with $n_{e0}\approx$6x$10^{19}$ $m^{-3}$, $T_{e0}\approx$12 keV and $T_{i0}\approx$26 keV.

## ACKNOWLEDGEMENTS

The authors appreciate the contributions of Task Force P from JET and the specific contributions of M. Zarnstorff, G. Schmidt from PPPL and of B. Lloyd, C. Warwick, C. Hunt from the Task agreement with UKAEA. They have been very valuable for the work and analysis presented in this paper.

## REFERENCES

[1] The JET Team, Nuclear Fusion **30** (1990), 187.

[2] Lazarus, E.A. et al., Plasma Physics and Controlled Nuclear Fusion Research, Proceedings 15th International Conference, Sevilla, 1994, Volume 1, IAEA Vienna (1995) 609.

[3] Tubbing B, et al., Nuclear Fusion **31** (1991), 839.

[4] Hugon, M. et al., Nuclear Fusion **32** (1992), 33.

[5] Levington, F.M. et al., Physics Review Letters **75** (1995), 4417.

[6] Strait, E.J. et al., Physical Review Letters **75** (1995), 4421.

[7] Fujita, T. et. al., Plasma Physics and Controlled Nuclear Fusion Research, Proceedings 16th International Conference, Montreal, 1996, IAEA-CN-64/A1-4.

[8] Söldner, F.X. and the JET Team, Plasma Physics and Controlled Nuclear Fusion Research, Proceedings 15th International Conference, Sevilla, 1994, IAEA-CN-60/A3-I2.

[9] Bell, R.E. et al., Physics Review Letters **60** (1988), 1294.

[10] Litaudon, X. et al., Plasma Physics and Controlled Fusion **38** (1996), 1603.

[11] Jacquinot, J. and the JET Team, Plasma Physics and Controlled Nuclear Fusion Research, Proceedings 16th International Conference, Montreal, 1996, IAEA-CN-64/O1-4.

[12] Gormezano, C. and the JET Team, Plasma Physics and Controlled Nuclear Fusion Research, Proceedings 16th International Conference, Montreal, 1996, IAEA-CN-64/A5-5.

[13] Goldston, R.J. et al., Journal of Computational Physics **43** (1981) 61.

[14] Cottrell, G.A. et al., 24th European Conference on Controlled Fusion and Plasma Physics, Berchtesgaden, 1997, to be published.

[15] Lao, L.L. et al., Nuclear Fusion **30** (1990), 1035.

[16] Huysmans, G.T.A. et al., 24th European Conference on Controlled Fusion and Plasma Physics, Berchtesgaden, 1997, to be published.

[17] Söldner, F.X. et al., 24th European Conference on Controlled Fusion and Plasma Physics, Berchtesgaden, 1997, to be published in Plasma Physics and Controlled Fusion.

[18] Rimini, F.G., private communication, and Rimini, F.G. et al, 24th European Conference on Controlled Fusion and Plasma Physics, Berchtesgaden, 1997, to be published.

[19] Strait, E.J. et al., 23rd European Conference on Controlled Fusion and Plasma Physics, Kiev, 1996, Volume III, 1493.